

Isothermal microcalorimetry provides new insights into biofilm variability and dynamics

Monika Astasov-Frauenhoffer¹, Olivier Braissant^{2,3}, Irmgard Hauser-Gerspach¹, Alma U. Daniels², Roland Weiger⁴ & Tuomas Waltimo¹

¹Institute of Preventive Dentistry and Oral Microbiology, School of Dental Medicine, University of Basel, Basel, Switzerland; ²Laboratory of Biomechanics and Biocalorimetry, c/o Biozentrum/Pharmazentrum, University of Basel, Basel, Switzerland; ³Department of Urology, University Hospital Basel, Basel, Switzerland; and ⁴Clinic for Periodontology, Endodontology and Cariology, University of Basel, Basel, Switzerland

Correspondence: Monika Astasov-Frauenhoffer, Institute of Preventive Dentistry and Oral Microbiology, School of Dental Medicine, University of Basel, Hebelstrasse 3, 4056 Basel, Switzerland. Tel.: +41 (0)61 267 25 98; fax: +41 (0)61 267 26 58; e-mail: m.astasov-frauenhoffer@unibas.ch

Received 1 June 2012; revised 13 August 2012; accepted 3 September 2012.

DOI: 10.1111/1574-6968.12007

Editor: Gilbert Shama

Keywords

oral biofilm; metabolic activity; heat flow; scanning electron microscopy; fluorescence *in situ* hybridization; isothermal microcalorimetry.

Abstract

The purpose of this study was to investigate a three-species *in vitro* biofilm with peri-implantitis-related bacteria for its variability and metabolic activity. *Streptococcus sanguinis*, *Fusobacterium nucleatum*, and *Porphyromonas gingivalis* were suspended in simulated body fluid containing 0.2% glucose to form biofilms on polished, protein-coated implant-grade titanium disks over 72 h using a flow chamber system. Thereafter, biofilm-coated disks were characterized by scanning electron microscopy and fluorescence *in situ* hybridization/confocal laser scanning microscopy. To assess metabolic activity within the biofilms, their heat flow was recorded for 480 h at 37 °C by IMC. The microscopic methods revealed that the total number of bacteria in the biofilms varied slightly among specimens ($2.59 \times 10^4 \pm 0.67 \times 10^4$ cells mm⁻²), whereas all three species were found constantly with unchanged proportions (*S. sanguinis* 41.3 ± 4.8%, *F. nucleatum* 17.7 ± 2.1%, and *P. gingivalis* 41.0 ± 4.9%). IMC revealed minor differences in time-to-peak heat flow (20.6 ± 4.5 h), a trend consistent with the small variation in bacterial species proportions as shown by microscopy. Peak heat flow (35.8 ± 42.6 µW), mean heat flow (13.1 ± 22.0 µW), and total heat over 480 h (23.5 ± 37.2 J) showed very high variation. These IMC results may be attributed to differences in the initial cell counts and relative proportions of the three species, their distribution and embedment in exopolysaccharide matrix on the test specimens. The present results provide new insights into variability and dynamics of biofilms on titanium disks, aspects that should be explored in future studies of dental surfaces.

Introduction

Biofilms can be described as communities of microbiota with associated extracellular polymeric matrix on a substrate. Microorganisms within such biofilms respond to local environmental conditions in various ways, such as altering their gene-expression patterns or undertaking physiological activities to adapt to a particular condition/location within the biofilm. This reveals heterogeneities within the bacterial population (Stewart & Franklin, 2008). Furthermore, as the microbial cells adapt their growth within surface-associated communities, they often change their characteristic shape and size from those that they exhibit during planktonic growth, thus making their

microscopic identification challenging (Costerton, 1999; Webster *et al.*, 2004). Natural variants within biofilms increase tolerance of antimicrobial agents (Drenkard & Asubel, 2002) and help to adapt to environmental conditions (Klein *et al.*, 2010).

Well-developed biofilms on dental implant surfaces cause peri-implantitis, an infection-induced inflammation that is one of the main causes of dental implant failure (Paquette *et al.*, 2006). Due to the complex nature of the supragingival/subgingival implant-associated biofilm formation, *in vitro* modeling is challenging. However, it may offer an efficient approach for studying biomaterials and biofilms, including their responses to therapeutic interventions. Recent reports on early colonization and biofilm

formation on implant surfaces indicate the urgent need for further developments in dental materials science and infection control (Quirynen *et al.*, 2006; Fürst *et al.*, 2007; Heuer *et al.*, 2007; Salvi *et al.*, 2008; Pye *et al.*, 2009; Mombelli & Décaillot, 2011).

Microscopic analyses have proven to be invaluable tools in describing biofilms in terms of their structure and association with a surface. Scanning electron microscopy (SEM) allows a high-resolution and magnification. However, SEM cannot be used to visualize bacteria embedded in the exopolysaccharide matrix (EPS) (Marrie *et al.*, 1982). As a complement to SEM, fluorescence *in situ* hybridization (FISH) combined with confocal laser scanning microscopy (CLSM) allows the observations of the spatial organization and quantification of bacterial biofilms using 16S rRNA gene-labeled probes even within EPS matrix (Amann, 1995; Paster *et al.*, 1998; Schwartz *et al.*, 2003; Thurnheer *et al.*, 2004; Al-Ahmad *et al.*, 2009). In various studies over the last decade, these methods have facilitated direct observations to characterize the bacterial distribution within oral biofilms (Wecke *et al.*, 2000; Thurnheer *et al.*, 2004; Dige *et al.*, 2009; Schaudinn *et al.*, 2009). Neither of these microscopic approaches, however, is sufficient to give real-time information about the dynamics of the metabolic activity and biomass formation within biofilms; rather, they only provide sequential periodic 'snapshots,' over time, of the structure and composition of the biofilm.

Isothermal microcalorimetry (IMC) is a highly sensitive analytical tool that provides, in real time, the progress of a chemical and physical process. All such processes produce or consume heat. The heat flow ($W = J s^{-1}$) is proportional to the reaction rate, and total heat over time (J) is a measurement of the extent of the process. IMC captures heat flow in the microwatt (μW) range and enables detection of the metabolic heat evolved from ca. 10 000 mammalian cells or ca. 100 000 bacteria (Braissant *et al.*, 2010). Thus, IMC has the potential to provide real-time quantitative data on metabolic activity, aggregation, and biomass formation in biofilms *in situ*. The sensitivity of IMC has been exploited in evaluating metabolism and growth of living cells in culture in medical and environmental microbiology (Howell *et al.*, 2012). While IMC has been applied to study the co-aggregation of different strains of biofilm-forming bacteria (Postollec *et al.*, 2003), studies that focus on the use of this technique for investigating *in vitro* multispecies biofilms are scarce.

The purpose of this study was to characterize a peri-implantitis-related biofilm by well-established commonly used microscopic methods and to complement this information using IMC to determine various measures of the metabolic activity. A three-species biofilm was allowed to form on surfaces of protein-coated titanium disks in a

newly developed anaerobic flow chamber system. The selected bacterial species were an early colonizer, *Streptococcus sanguinis*; a pathogenic bridging organism, *Fusobacterium nucleatum*; and a common periodontal and peri-implant pathogen, *Porphyromonas gingivalis* (Quirynen *et al.*, 2006; Fürst *et al.*, 2007; Heuer *et al.*, 2007).

Materials and methods

Bacterial suspensions

Streptococcus sanguinis (DSM 20068), *F. nucleatum* (ATCC 10953), and *P. gingivalis* (DSM 20709) were used for the biofilm formation. A 10 μL inoculum of *S. sanguinis* in skim milk solution (stored at $-20^{\circ}C$) was suspended in 5 mL Schaedler broth (BBLTM, Becton Dickinson, Basel, Switzerland) and incubated aerobically at $37^{\circ}C$ for 8 h. The bacterial suspension was used as an inoculum for a new subculture (1 : 50), which was incubated aerobically at $37^{\circ}C$ for 16 h. The culture was ultrasonicated for 30 s (22.5 W; Vibracell, Sonics & Materials, Newtown, CT), centrifuged at 5700 g for 5 min at room temperature, washed with physiological saline, and harvested by centrifugation. The *S. sanguinis* cells were resuspended in simulated body fluid (Cho *et al.*, 1995) to a density of $1.1 \times 10^8 \pm 6.2 \times 10^7$ CFU mL⁻¹. *Fusobacterium nucleatum* and *P. gingivalis* were maintained in Microbank[®] blue vials (Chemie Brunschwig AG, Basel, Switzerland) at $-70^{\circ}C$. One pearl of each frozen culture was inoculated into 10 mL thiogluconate aliquots (Biomerieux SA, Geneva, Switzerland), enriched with 5 μg mL⁻¹ hemin (Fluka, Buchs, Switzerland) and 0.5 μg mL⁻¹ menadione (VWR International, Dietikon, Switzerland), and incubated anaerobically at $37^{\circ}C$ for 96 h. The cultures were harvested; *F. nucleatum* and *P. gingivalis* were suspended to a density of $3.2 \times 10^7 \pm 1.9 \times 10^6$ CFU mL⁻¹ and $2.1 \times 10^9 \pm 9.3 \times 10^8$ CFU mL⁻¹, respectively.

Anaerobic flow chamber

Details and uses of the flow chamber system have been presented previously (Weiger *et al.*, 1999; Decker *et al.*, 2003a, b, 2008; Hauser-Gerspach *et al.*, 2007; Meier *et al.*, 2008; Vig Slensters *et al.*, 2008); thus only brief descriptions of its main parts are given here. The system consists of an anaerobic flow chamber (Minucells, Bad Abbach, Germany) with (1) a test specimen mounted with its test surface not facing the flow direction; (2) a Teflon[®] dispenser (Multimed GmbH, Kirchheim unter Teck, Germany) containing the bacterial suspension; and (3) a peristaltic pump (Spetec GmbH, Erding, Germany) with an integrated speed controller. In this study, the system was modified to mimic conditions related to peri-implantitis, namely an anaerobic

atmosphere and a slow-flowing, nutrient-poor environment containing three different strains of peri-implantitis-related bacteria. Specifically, the circulating bacteria were allowed to adhere to the protein-coated titanium specimens under anaerobic conditions (MACS MG; Don Whitley Scientific Ltd; atmosphere of 80% N₂, 10% H₂ and 10% CO₂) at 37 °C for 72 h.

Biofilm formation

Sterile polished disks of commercially pure titanium (Grade 2, ASTM F-67), 5 mm diameter and 1 mm thickness, with a mean surface roughness of 120 nm (Straumann AG, Basel, Switzerland), were sterilized by steam autoclaving and gamma irradiation and used as substrates. The disks were placed for 15 min in freshly mixed serum/saliva mixture (1 : 10) prior to each experiment in order to allow protein pellicle formation (Hauser-Gerspach *et al.*, 2007). Fasting stimulated saliva of three healthy volunteers was homogenized, filtered through a 70- μ m filter (Cell Strainer; Becton Dickinson), and centrifuged at 22 000 g for 45 min at 4 °C. The supernatant was filter-sterilized (45 and 0.22 μ m; Millex-HV and Millex-GV respectively; Millipore, Switzerland) and mixed with pooled serum (Blutspendezentrum, Basel, Switzerland).

The protein-coated substrates were placed in the anaerobic flow chamber, 0.2% glucose was added to the bacterial suspension, and the suspension was circulated at 0.8 mL min⁻¹ for 72 h. To compensate for the decrease in pH of the bacterial suspension (7.26 \pm 0.07 to 4.84 \pm 0.21), it was renewed in 24-h intervals. After 72 h, the biofilm-coated titanium disks were evaluated using SEM, CLSM, and IMC.

SEM

The biofilms were fixed overnight in 2% glutaraldehyde solution (Sigma, Buchs, Switzerland), washed once with PBS, and dehydrated in stepwise increasing concentrations of ethanol – 30%, 50%, 70%, 90%, 2 \times 100% for 10 min each. The samples ($n = 3$) were then critical-point-dried and coated with 10 nm of gold and examined (Fei Nova NanoSEM 230[®], Eindhoven, the Netherlands).

FISH and CLSM

Oligonucleotide DNA probes, labeled at the 5'-end with Cy3 and Cy5 or with 6-carboxyfluorescein (FAM) and additionally labeled at the 3'-end (Microsynth AG, Balgach, Switzerland), are listed with their sequences and specificities in Table 1. Appropriate probe sequences for the specific detection of each bacterial strain in the biofilm have been described previously (Paster *et al.*, 1998; Thurnheer *et al.*, 2004; Guggenheim *et al.*, 2009).

The biofilms were fixed in 4% paraformaldehyde (Sigma) for 1 h at 4 °C and washed once with PBS. Thereafter, the biofilm-associated microorganisms were permeabilized by exposure to lysozyme (Sigma; 70 000 U mL⁻¹) for 2 min at room temperature and rinsed with physiological saline. FISH was carried out using a modification of a method previously described (Thurnheer *et al.*, 2004). The biofilms were pre-incubated for 15 min at 48 °C in final hybridization buffer (0.9 M NaCl, 20 mM L⁻¹ Tris-HCl pH 7.5, 0.01% SDS) containing 30% formamide and then placed for 3 h at 48 °C in the same solution with the oligonucleotide probes added (5 μ g mL⁻¹ for STR405 and LNA-Pging, 15 μ g mL⁻¹ for FUS664). After hybridization, the biofilms were immersed for 15 min at 48 °C in washing buffer (102 mM L⁻¹ NaCl, 20 mM L⁻¹ Tris-HCl 7.5, 5 mM L⁻¹ EDTA, 0.01% SDS). Thereafter, the disks were embedded upside-down in 10 μ L Mowiol mounting solution and stored at room temperature in the dark at least 6 h. Biofilms were examined using a Leica SP5[®] microscope (Leica, Wetzlar, Germany) fitted with three lasers: He-Ne, argon and DPSS. Filters were set to 490–530 nm for FAM, 570–610 nm for Cy3, and 650–730 nm for Cy5. The fluorescence signal from Cy5 was assigned to blue color for better differentiation from Cy3. Confocal images were obtained using a 63 \times (numeric aperture 1.4) oil immersion objective. Each biofilm was scanned at three random positions at the center of the disk. Z-direction series were generated by vertical optical sectioning at every position with the thickness of the slices set to 0.3 μ m. Proprietary Leica confocal software was used to acquire digital images of 1024 \times 1024 pixels in size that were the average of 32 frames. The counts of the bacteria in the biofilm were made using image analysis software (Olympus AG,

Table 1. Characteristics of 16S rRNA gene-directed oligonucleotide probes used for FISH (underlined bases have locked ribose conformation)

Probe	Tag	Target	Sequence (5' \rightarrow 3')	Reference
STR405	Cy5	<i>S. sanguinis</i>	TAG CCG TCC CTT TCT GGT	(Thurnheer <i>et al.</i> , 2004)
FUS664	FAM2	<i>F. nucleatum</i>	CTT GTA GTT CCG CYT ACC TC	(Paster <i>et al.</i> , 1998)
LNA-Pging	Cy3	<i>P. gingivalis</i>	GTT TTC ACC ATC <u>M</u> G <u>T</u> <u>C</u> A <u>T</u> <u>C</u>	(Guggenheim <i>et al.</i> , 2009)

Volketswil, Switzerland) and verified manually on random views to exclude possible errors due to not counting bacteria present in bundles. The experiment was repeated twice, resulting in six disks that were scanned at three random position in the central area.

IMC

Three milliliters of Columbia agar (BBL™; Becton Dickinson) supplemented with 5% human blood (Blutspendezentrum), $5 \mu\text{g mL}^{-1}$ hemin (Fluka, Buchs, Switzerland), and $0.5 \mu\text{g mL}^{-1}$ menadione (VWR International, Dietikon, Switzerland) were placed in sterile IMC ampoules and incubated anaerobically for 48 h. Specimens with the biofilms were placed in ampoules, enabling continuous contact between the biofilm and the agar. A sterile titanium disk with no biofilm on it served as the negative control. Each of the ampoules was immediately sealed under anaerobic conditions and inserted into one of the individual microcalorimeters in the 48-microcalorimeter instrument used (TAM 48®; TA Instruments, New Castle, DE). The heat flow ($\mu\text{J s}^{-1} = \mu\text{W}$), due to the heat given up during bacterial activity in the biofilm ($n = 24$), was recorded continuously for 480 h. From the data, the following parameters were determined: time-to-peak heat flow, peak

heat flow, mean heat flow (that is, heat flow averaged over the period, 72–420 h, as during this time it stayed on a stable plateau level after reaching the peak heat flow), and total heat produced up to 480 h (computed as the integral of the heat-flow-vs.-time curve between 0 and 480 h).

Statistical analysis

For each of the four IMC parameters determined, the median, mean, and standard deviation were computed. Test of significance was conducted using the Kruskal–Wallis analysis of variance method and a commercially available software package (STATA Statistical Software, release 16; StataCorp, College Station, TX). Significance was denoted at $P < 0.05$.

Results

SEM revealed that a biofilm was present over the entire surface of a protein-coated titanium disk (Fig. 1a), although minor variations were observed in the density and areas covered by the EPS matrix (Fig. 1b).

FISH/CLSM showed bundles of *F. nucleatum* cells that formed the framework of the biofilm in which both coccal species were observed to bind (Fig. 2). Hardly, any

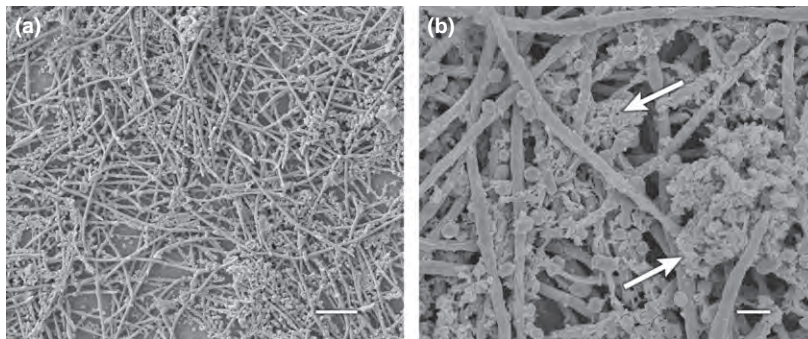


Fig. 1. SEM scans of 72-h-old *in vitro* three-species biofilm. Bars on the pictures indicate $5 \mu\text{m}$ on (a) and $1 \mu\text{m}$ on (b). A continuous biofilm formation is detected all over the surface (a); in detailed view of (a), the formation of EPS is shown on (b) with arrows.

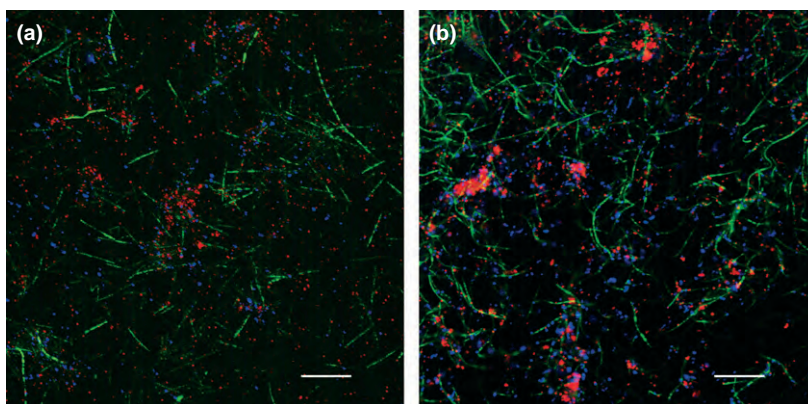


Fig. 2. Biofilms detected by FISH/CLSM – *Streptococcus sanguinis* shown in blue (STR405-Cy5), *Fusobacterium nucleatum* in green (FUS664-FAM2) and *Porphyromonas gingivalis* in red (LNA-Pging-Cy3). The variability in the total counts of the bacteria is shown on panels (a) and (b). Bar indicates $50 \mu\text{m}$.

co-adherence between the two coccal species was detected. While the relative proportions of the bacterial species stayed unchanged within the biofilms, the total bacterial count showed significant differences ($P < 0.05$); however, the biological meaning of the minor differences in total counts is doubtful (Table 2).

A typical IMC heat-flow-vs.-time plot is given in Fig. 3. In 17 of 24 samples, after the heat flow reached a peak, it gradually reduced and finally returned to baseline value. In each of the other seven samples, however, after the heat flow reached a peak, it did not reduce to baseline value but remained at a high plateau. While the variability in the time-to-reach peak, heat flow is low, each of the other three parameters determined showed large variability (Table 3).

Table 2. Bacterial proportions and total counts of *Streptococcus sanguinis*, *Fusobacterium nucleatum* and *Porphyromonas gingivalis* in the 72-h-old biofilm detected by FISH/CLSM

Species	Strain	Proportion (%)	Total cell count (cells mm ⁻²)
<i>S. sanguinis</i>	DSM 20068	41.3 ± 4.8	$1.07 \times 10^4 \pm 2.97 \times 10^3$
<i>F. nucleatum</i>	ATCC 10953	17.7 ± 2.1	$4.90 \times 10^3 \pm 2.08 \times 10^3$
<i>P. gingivalis</i>	DSM 20709	41.0 ± 4.9	$1.06 \times 10^4 \pm 4.13 \times 10^3$

Mean ± SD are given ($n = 6$).

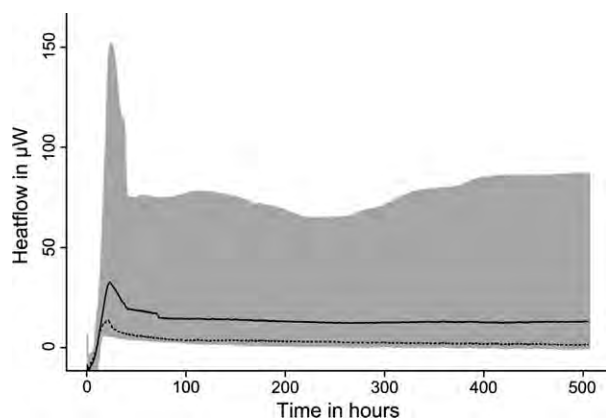


Fig. 3. Typical heat flow-vs.-time curve, as obtained using IMC. The range of the curve is shown as the gray area, the mean curve is the continuous curve and median curve is the dotted curve ($n = 24$).

Table 3. Summary of IMC results ($n = 24$)

	Time-to-peak heat flow (h)	Peak heat flow (µW)	Mean heat flow (µW)	Total heat produced (J)
Median	20.5	14.9	2.7	5.5
Mean	20.6	35.8	13.1	23.5
Standard deviation	4.5	42.6	22.0	37.2

Discussion

Microscopic analyses have proven to be invaluable tools in describing biofilms in terms of their structure and association with a surface; however, no real-time information about the dynamics of the metabolic activity and biomass formation can be obtained. The present study is the first of its kind characterizing a multispecies *in vitro* biofilm using both well-established microscopic methods (SEM and FISH/CLSM) and a very sensitive calorimetric method (IMC).

Imaging by SEM was used to gain the first overview of the formed biofilm. As intended, the scans revealed biofilms that covered the entire surface with bacteria partially embedded in EPS, indicating that 0.2% glucose (Tenuta *et al.*, 2006; Filoche *et al.*, 2007) was sufficient to induce EPS formation. In addition, SEM showed that *F. nucleatum* served as the central 'bridging organism' or framework in the biofilm architecture, demonstrating inter- and intraspecies cellular binding (Lancy *et al.*, 1983; Kaplan *et al.*, 2009; Merritt *et al.*, 2009). SEM was not able to distinguish between the two coccal species present in the biofilm partly because of their similar shape and size, and partly because of embedding in EPS.

FISH/CLSM allowed the discrimination between *S. sanguinis* and *P. gingivalis* and determination of the relative proportions of all three species. A partially heterogeneous architecture of the biofilm, which may be due competitive binding, was observed. However, the distribution of the relative proportions of the three species in all experiments stayed unchanged.

The heat flow at a given time (as determined using IMC) was a measure of metabolic activities of all bacteria present, and it thus declines correspondingly if bacterial activity diminishes. Similarly, heat over time (i.e. the integral of the heat flow) is a proxy for the growth curve and approaches a maximum when metabolic activity decreases (Braissant *et al.*, 2010). This metabolic decline and asymptotic biomass accumulation pattern is due to changes in the IMC ampoule internal environment that occur during bacterial metabolism; that is, exhaustion of available nutrients or electron acceptors or build up of metabolic waste products. The pattern of rise and decline of the metabolic activity of the biofilm was seen in the first 50 h (Fig. 3) exhibiting similarities in the behavior of the biofilm to common liquid or solid culture studies (Braissant *et al.*, 2010). Thus, cumulative heat correlates with cumulative bacterial biomass only during this early part when the biofilm still grows and until heat flow peak is reached. Once the heat flow has stabilized at a constant level, the accumulation of heat is most probably not related to a net increase in bacterial numbers and production of fresh biomass, but, rather, to metabolic activities

related to maintenance of the mature biofilm and survival of the present cells. Alternatively, it can be hypothesized that during this steady state of the heat flow, growth rate is equal to bacterial death rate, resulting in a stable metabolically active bacterial population. This latter hypothesis is in line with the first one if equally low growth and death rates are considered.

In the present study, between 72–480 h ca. 70% of the samples ($n = 17$) showed a low steady state heat flow comprised between 0.8 and 1.8 μW , whereas in the remaining 30% ($n = 7$), the values were found much higher (reaching from 8.6 to 86.0 μW). Assuming a heat flow of 2 pW per active bacterial cell (James, 1987), we calculated the number of active bacteria in the biofilm. This suggests that in the present samples showing the lowest steady state heat flow, ca. 4×10^5 to 9×10^5 bacteria remained active on the surface of the titanium disk (5 mm²), whereas this number is up to 4.3×10^7 in the samples having the highest heat flow. This result emphasizes major variability within biofilms that appear similar in microscopic analyses. On the other hand, the time required to reach the maximum heat flow showed only moderate specimen-to-specimen variability. This can be understood as a consequence of the static conditions of measurement – constant temperature, sealed and unstirred ampoules, a fixed initial chemical environment, plus, as shown by FISH/CLSM, unchanged relative initial proportions of the three bacteria (Table 2).

In contrast to the time required to reach the maximum heat flow peak, each of the three parameters computed from the IMC data varied widely (Table 3), showing that biofilm maturation rapidly diverges between originally similar samples. These results indicate heterogeneity of the aggregate metabolic activity of all bacteria present and reflect the differences in remaining active cells after 480 h. These findings regarding the heat flow and the total heat must, by definition, reflect the total number of bacteria present at the time or the time interval over which the parameters are calculated. At this point, it should be remembered that, in contrast to microscopic analyses that provide generalized data based on number of scans taken, IMC allows the measurement of the whole surface of the test specimen harboring the biofilm. Therefore, the variability of the IMC results may be explained by differences in the initial cell counts and bacterial distributions within the biofilm on the titanium disks that cannot be detected by microscopy where the whole surface area cannot be studied in detail.

In conclusion, (1) three-species biofilm formed on protein-coated titanium was documented by SEM and FISH/CLSM; specifically, the species present, their proportions, and their approximate surface distribution were determined; (2) IMC detected a surprisingly high variability

within biofilms as the measurement includes the whole surface area harboring the biofilm rather than generalized data based on number of areas scanned; (3) these new insights may be beneficial, and, thus, should be considered in future research into biofilms on dental surfaces.

Acknowledgements

We thank Prof. Dr. Rudolf Gmür and Dr. Thomas Thurnheer (Institute of Oral Biology, University of Zurich), for fruitful discussions on FISH; Evi Bieler and Dr. Markus Dürrenberger (Microscopy center, University of Basel, Switzerland), for assistance with microscopic analyses; and Straumann AG (Basel, Switzerland), for providing the titanium disks. The manuscript was partially supported by Swiss Dental Association grant SSO246-09.

References

- Al-Ahmad A, Follo M, Selzer A-C, Hellwig E, Hannig M & Hannig G (2009) Bacterial colonization of enamel *in situ* investigated using fluorescence *in situ* hybridization. *J Med Microbiol* **58**: 1359–1366.
- Amann RI (1995) *In situ* identification of microorganisms by whole cell hybridization with rRNA-targeted nucleic acid probes. *Molecular Microbial Ecology Manual*, Vol. 3.3.6. Kluwer Academic Publishers, Bodrecht, The Netherlands, pp. 1–15.
- Braissant O, Wirz D, Goepfert B & Daniels AU (2010) Use of isothermal microcalorimetry to monitor microbial activities. *FEMS Microbiol Lett* **303**: 1–8.
- Cho SB, Nakanishi K, Soga N, Ohtsuki C, Nakamura T, Kitsugi T & Yamamuro T (1995) Defence of apatite formation on silica gel on its structure: effect of heat treatment. *J Am Ceram Soc* **78**: 1769–1774.
- Costerton JW (1999) Introduction to biofilm. *Int J Antimicrob Agents* **11**: 217–221.
- Decker EM, Weiger R, Wiech I, Heide PE & Brex M (2003a) Comparison of antiadhesive and antibacterial effects of antiseptics on *Streptococcus sanguinis*. *Eur J Oral Sci* **111**: 144–148.
- Decker EM, Weiger R, von Ohle C, Wiech I & Brex M (2003b) Susceptibility of planktonic versus attached *Streptococcus sanguinis* cells to chlorhexidine. *Clin Oral Investig* **7**: 98–102.
- Decker EM, Maier G, Axmann D, Brex M & von Ohle C (2008) Effect of xylitol/chlorhexidine versus xylitol or chlorhexidine as single rinses on initial biofilm formation of cariogenic streptococci. *Quintessence Int* **39**: 17–22.
- Dige I, Nyengaard JR, Kilian M & Nyvad B (2009) Application of stereological principles for quantification of bacteria in intact dental biofilms. *Oral Microbiol Immunol* **24**: 69–75.
- Drenkard E & Asubel FM (2002) *Pseudomonas* biofilm formation and antibiotic resistance are linked to phenotypic variation. *Nature* **416**: 740–743.

- Filoché SK, Soma KJ & Sissons CH (2007) Caries-related plaque microcosm biofilms developed in microplates. *Oral Microbiol Immunol* **22**: 73–79.
- Fürst MM, Salvi GE, Lang NP & Persson GR (2007) Bacterial colonization immediately after installation on oral titanium implants. *Clin Oral Implants Res* **18**: 501–508.
- Guggenheim B, Gmür R, Galicia JC, Stathopoulou PG, Benakanakere MR, Meier A, Thurnheer T & Kinane DF (2009) *In vitro* modeling of host-parasite interactions: the 'subgingival' biofilm challenge of primary human epithelial cells. *BMC Microbiol* **9**: 280–292.
- Hauser-Gerspach I, Kulik EM, Weiger R, Decker EM, Von Ohle C & Meyer J (2007) Adhesion of *Streptococcus sanguinis* to dental implant and restorative materials *in vitro*. *Dent Mater J* **26**: 361–366.
- Heuer W, Elter C, Demling A, Neumann A, Suerbaum S, Hannig M, Heidenblut T, Bach FW & Stiesch-Scholz M (2007) Analysis of early biofilm formation on oral implants in man. *J Oral Rehabil* **34**: 377–382.
- Howell M, Wirz D, Daniels AU & Braissant O (2012) Application of a microcalorimetric method for determining drug susceptibility in mycobacterium species. *J Clin Microbiol* **50**: 16–20.
- James AM, ed (1987) *Thermal and Energetic Studies of Cellular Biological Systems*. Wright Publ, Bristol, UK, pp. 147–166.
- Kaplan CW, Lux R, Haake SK & Shi W (2009) The *Fusobacterium nucleatum* outer membrane protein RadD is an arginine-inhibitable adhesin required for inter-species adherence and the structured architecture of multispecies biofilm. *Mol Microbiol* **71**: 35–47.
- Klein MI, DeBaz L, Agidi S, Lee H, Xie G, Lin AH, Hamaker BR, Lemos JA & Koo H (2010) Dynamics of *Streptococcus mutans* transcriptome in response to starch and sucrose during biofilm development. *PLoS ONE* **5**: e13478.
- Lancy PJ, Dirienzo JM, Appelbaum B, Rosan B & Holt SC (1983) Corn-cob formation between *Fusobacterium nucleatum* and *Streptococcus sanguis*. *Infect Immun* **40**: 303–309.
- Marrie TJ, Nelligan J & Costerton JW (1982) A scanning and transmission electron microscopic study of an infected endocardial pacemaker lead. *Circulation* **66**: 1339–1341.
- Meier R, Hauser-Gerspach I, Lüthy H & Meyer J (2008) Adhesion of oral streptococci to all-ceramics dental restorative materials *in vitro*. *J Mater Sci Mater Med* **19**: 3249–3253.
- Merritt J, Niu G, Okinaga T & Qi F (2009) Autoaggregation response of *Fusobacterium nucleatum*. *Appl Environ Microbiol* **75**: 7725–7733.
- Mombelli A & Décalet F (2011) The characteristics of biofilms in peri-implant disease. *J Clin Periodontol* **38**: 203–213.
- Paquette DW, Brodala N & Williams RC (2006) Risk factors for endosseous dental implant failure. *Dent Clin North Am* **50**: 361–374.
- Paster BJ, Bartoszyk I & Dewhirst FE (1998) Identification of oral streptococci using PCR-based, reverse-capture, checkerboard hybridization. *Methods Cell Sci* **20**: 223–231.
- Postollec F, Norde W, van der Mei HC & Busscher HJ (2003) Enthalpy of interaction between coaggregating and non-coaggregating oral bacterial pairs—a microcalorimetric study. *J Microbiol Methods* **55**: 241–247.
- Pye AD, Lockhart DEA, Dawson MP, Murray CA & Smith AJ (2009) A review of dental implants and infection. *J Hosp Infect* **72**: 104–110.
- Quirynen M, Vogels R, Peeters W, van Steenberghe D, Naert I & Haffajee A (2006) Dynamics of initial subgingival colonization of 'pristine' peri-implant pockets. *Clin Oral Implants Res* **17**: 25–37.
- Salvi GE, Fürst MM, Lang NP & Persson GR (2008) One-year bacterial colonization patterns of *Staphylococcus aureus* and other bacteria at implants and adjacent teeth. *Clin Oral Implants Res* **19**: 242–248.
- Schaudinn C, Carr G, Gorur A, Jaramillo D, Costerton JW & Webster P (2009) Imaging of endodontic biofilms by combined microscopy (FISH/cLSM – SEM). *J Microsc* **235**: 124–127.
- Schwartz T, Hoffmann S & Obst U (2003) Formation of natural biofilms during chlorine dioxide and u.v. disinfection in a public drinking water distribution system. *J Appl Microbiol* **95**: 591–601.
- Stewart PS & Franklin MJ (2008) Physiological heterogeneity in biofilms. *Nat Rev Microbiol* **6**: 199–210.
- Tenuta LM, Ricomini Filho AP, Del Bel Cury AA & Cury JA (2006) Effect of sucrose on the selection of mutans streptococci and lactobacilli in dental biofilm formed *in situ*. *Caries Res* **40**: 546–549.
- Thurnheer T, Gmür R & Guggenheim B (2004) Multiplex FISH analysis of a six-species bacterial biofilm. *J Microbiol Methods* **56**: 37–47.
- Vig Slensters T, Hauser-Gerspach I, Daniels AU & Fromm KM (2008) Silver coordination compounds as light-stable, nano-structured and anti-bacterial coatings for dental implant and restorative materials. *J Mater Chem* **18**: 5359–5362.
- Webster P, Wu S, Webster S, Rich KA & McDonald K (2004) Ultrastructural preservation of biofilms formed by non-typeable *Hemophilus influenzae*. *Biofilms* **1**: 165–182.
- Wecke J, Kersten T, Madela K, Moter A, Göbel UB, Friedmann A & Bernimoulin JP (2000) A novel technique for monitoring the development of bacterial biofilms in human periodontal pockets. *FEMS Microbiol Lett* **191**: 95–101.
- Weiger R, Decker EM, Krastl G & Brex M (1999) Deposition and retention of vital and dead *Streptococcus sanguinis* cells on glass surfaces in a flow-chamber system. *Arch Oral Biol* **44**: 621–628.